



Special Feature: Power Electronics for Hybrid Vehicles

Research Report

Simulation of Electric Field inside Human Body Induced by Magnetic Field around Vehicle with Wireless Power Transfer System

Toshiaki Watanabe and Masaya Ishida

Report received on May 10, 2017

■ABSTRACT■ We are developing a wireless power transfer (WPT) system that charges EV/PHEV wirelessly. In this WPT system, a magnetic resonant coupling method is used, in which power is transmitted and received by induction coils mounted to the ground and the bottom of the vehicle. There is concern about the health effects due to exposure to the human body of high-frequency leaked magnetic fields during power transmission. Regulations concerning electromagnetic field exposure to the human body are based on individual laws in each country, but it is common for legislation to reference guidelines of the ICNIRP, which is recognized internationally.

In this paper, we evaluate the influence on the human body from magnetic field leakage exposure by electromagnetic field simulation of wireless vehicle charging while a person is standing near the vehicle, which is a reasonable usage scenario. As a result, it was found that the magnetic field strength was 0.02 to 0.62 times the ICNIRP “reference level” and the induced electric field in the body was 0.003 to 0.027 times the ICNIRP “basic restriction”.

■KEYWORDS■ SPFD Method, WPT, Magnetic Coupling, ICNIRP, Dosimetry

1. Introduction

Wireless power transmission technology has been attracting attention since immediately after its announcement by MIT as a novel technology in 2007.⁽¹⁾ Automotive applications have been actively researched and developed in many research institutes in recent years. In addition, activities such as standardization for vehicle charging systems have been energetically carried out, and the technology is progressing steadily toward practical application. We are also working on development of wireless power charging system to be installed in electric vehicles (EVs) and plug-in hybrid EVs (PHEVs).

Since the vehicle wireless power transfer (WPT) system under development uses a magnetic coupling technique with induction coils, there is concern about the influence on the human body due to exposure to magnetic field leakage during high-power transmission. For this reason, it is important to properly evaluate the effect of magnetic field exposure on humans. However, most of the regulatory/standard values of each country at the frequency of 85 kHz band (81.39 kHz – 90 kHz), which is currently being considered for use in vehicle WPT systems, are provisional and not necessarily

appropriate in many cases. In order to respond to this situation, new regulatory/standard values are being legislated in compliance with the guidelines^(2,3) established by the International Commission on Non-ionizing Radiation Protection (ICNIRP), and similar activities are being conducted in Japan. Therefore, evaluation based on the ICNIRP guidelines becomes important in the near future.

In this paper, we evaluate the influence of leakage magnetic field exposure on the human body against the ICNIRP guidelines by electromagnetic field simulation, assuming that a WPT system is installed in an actual vehicle and a person is standing near the vehicle, which is a reasonable usage scenario. First, we quantitatively evaluate the level of the leakage magnetic field of the WPT system with respect to the “reference level” guidelines. Next, we quantitatively evaluate the induced electric field by the leakage magnetic field with respect to the “basic restriction” guidelines.

2. ICNIRP Guidelines for Human Body Protection from Magnetic Exposure

ICNIRP guidelines are intended to protect the

human body from exposure to electromagnetic fields. The ICNIRP issued the first guidelines, limited to static magnetic fields, in 1994. After that, several revisions were added, and a major revised version in the low- and intermediate-frequency band of 100 kHz or less was issued in 2010 (ICNIRP 2010).⁽³⁾

The members of the ICNIRP and the enactment process are in principle unpublished in order to strengthen independence from specific interested organizations. It is supported by the European Union and other governments and is also recognized as a cooperating organization by the World Health Organization. ICNIRP “above-background” guidelines are referred to as a safety standard for institutionalization or legislation in many countries.

The substance of ICNIRP 2010 is described below, focusing on the magnetic field exposure around the 100 kHz band associated with the WPT system. In ICNIRP 2010, two stages of standard values called the “reference level” and “basic restriction” are provided and are evaluated by magnetic field strength and in-body induced electric field strength, respectively (**Fig. 1**). The reference level is an allowable standard value in consideration of the possibility of actual measurement, and it can be applied to a uniform magnetic field distribution environment. Satisfaction of the more stringent “reference level” means automatic satisfaction of the basic restriction. On the other hand, the basic restriction is value which should not to be exceeded, and it is considered to be particularly applicable to a non-uniform magnetic field distribution environment. Since it has been reported that the leakage magnetic field from the coil of a car-mounted WPT system has a non-uniform distribution, with

a strong peak near the center of the coil,⁽⁴⁾ evaluation on the “basic restriction” is necessary.

3. Analysis Method

In this section, we describe the calculation methods used in the electromagnetic field simulation. The accuracy of the calculation model and the resolution of the calculation result required for the electromagnetic field simulation are greatly different between the magnetic field, which is the reference level, and the in-body induction electric field, which is the basic restriction. In the calculation of the induced electric field, ICNIRP 2010 recommends use of a numerical human body model comprising extremely small units, called voxels, of 2 mm × 2 mm or less. This is a high resolution requiring enormous resources, and it may be difficult to accomplish using a typical computer workstation. Therefore, we devised a more efficient calculation by using a two-step numerical calculation method,⁽⁵⁾ as shown in **Fig. 2**. The finite element method (FEM) was used to calculate the magnetic field distribution for the first step, and the scalar potential finite difference (SPFD) method⁽⁶⁾ was used to calculate the induced electric field in the human body for the second step. The SPFD method is based on quasi-static approximation, and it enables high-speed calculation. Here, it should be noted that the calculation region is large, including the entire vehicle in the first step, although it is possible to decrease the region to a narrow rectangular parallelepiped, including the human model, in the second step. The magnetic field distribution obtained in the first step becomes the

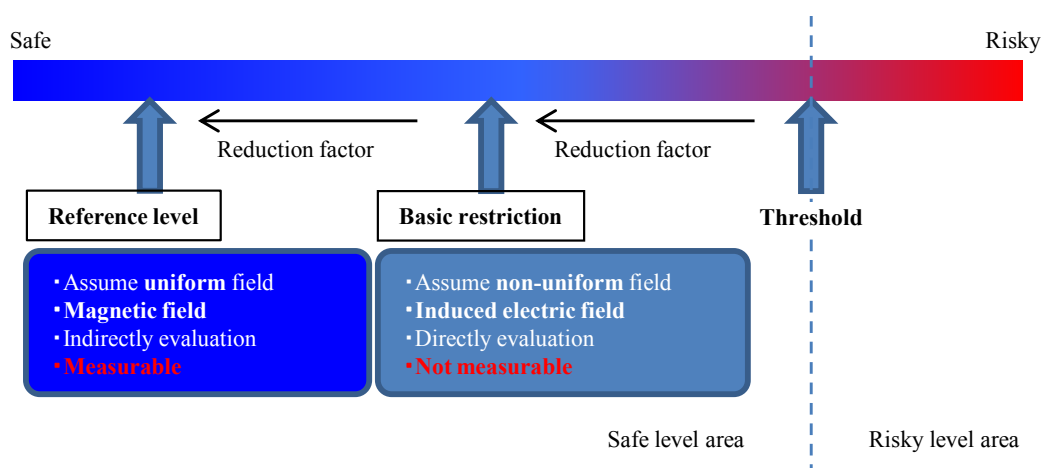


Fig. 1 Concept of ICNIRP guidelines.

input value for the SPFD method of the second step. For this reason, it is possible to minimize the precise calculation region of the induced electric field in the body and to greatly reduce the calculation resources. Calculation of the magnetic field strength distribution required in the second step is obtained by one calculation. Furthermore, since it is possible to determine the calculation condition of the second step after obtaining the magnetic field intensity distribution, searching for the worst case becomes easy, and unnecessary parameter setting can be avoided. The commercially available electromagnetic field simulator HFSSTM was used for the first step, and our original code was used for the second step.

4. Simulation Model and Calculation Condition of Evaluation

This section describes the magnetic coupling coil, the coil mounting condition, and the human body model used in the evaluation.

4.1 Shape of the Coil

Two coil shapes were selected: a solenoid coil (S coil, shown in Fig. 3) and a circular coil (C coil, shown in Fig. 4). Both coils consisted of metallic wire windings, a ferrite core, and a conductive plate. The primary coil for power transmission and the secondary coil for power reception have the same shape and the same size. In the S coil, wire is wound 10 turns around a ferrite core measuring $400 \times 400 \times 10$ mm. In the C coil, wire is wound in

a spiral pattern of 10 turns and tightly arranged on one side of a ferrite core measuring $550 \times 550 \times 10$ mm. The relative permeability μ_r of the ferrite core was 1800, and the conductivity σ of the metallic wire and the conductive plate was 5.8×10^7 S/m (equivalent to copper).

4.2 Car Body Model and Mounting Condition

The simulation model for the car body, the location of coil installation, and the coordinate system used in the calculation are shown in Fig. 5. We assumed the coil was installed in an ordinary passenger car having the dimensions shown in the figure. The secondary coil is mounted to the bottom of the vehicle, the primary coil is mounted to the floor below the secondary coil, and the gap g between the primary and secondary coils is 150 mm. In consideration of positional misalignment during parking, the maximum misalignment between the primary and secondary coils was 100 mm in the x direction and

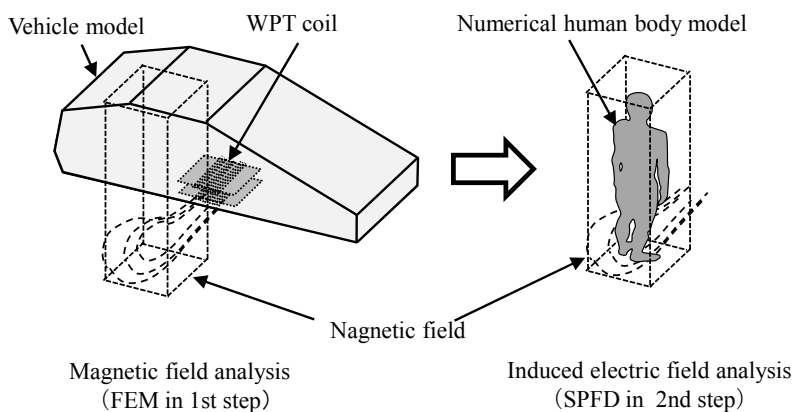


Fig. 2 Concept of two-step analysis method.

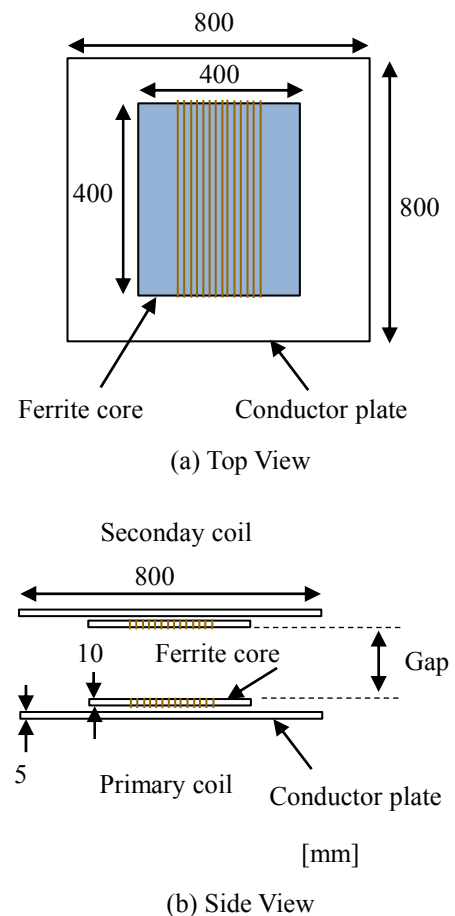


Fig. 3 Configuration of coil (S-coil).

75 mm in the y direction, as shown in **Fig. 6**. This corresponds to a shift in the left-right direction and the front-rear direction of the vehicle, respectively. The floor was assumed to be an infinitely perfect conductor.

Three coil mounting positions were used (front, center, and rear) and arranged at intervals of 1500 mm, as shown in **Fig. 7**.

4.3 Human Body Model

For the model of the human body, we used TARO,⁽⁷⁾ which is a numerical human body model of an adult male in databases provided by the National Institute of Information and Communication (NICT). In this model, the human body occupies a space of

$640 \times 320 \times 1732$ mm; this space is divided into 2 mm voxels; and each voxel is distinguished by material flags, such as skin, blood vessels, and organs. Physical properties, such as conductivity and relative permittivity for each of these flags, are given by Gabriel et al.⁽⁸⁾

4.4 Calculation Condition

The circuit topology of the WPT system used for this evaluation is shown in **Fig. 8**. We adopted the series-series type topology, which is a series resonance circuit for both primary and secondary coils. In **Fig. 8**, L_1 and L_2 are the inductances of the primary coil and the secondary coil, respectively, C_1 and C_2 are the capacitances of the primary coil and

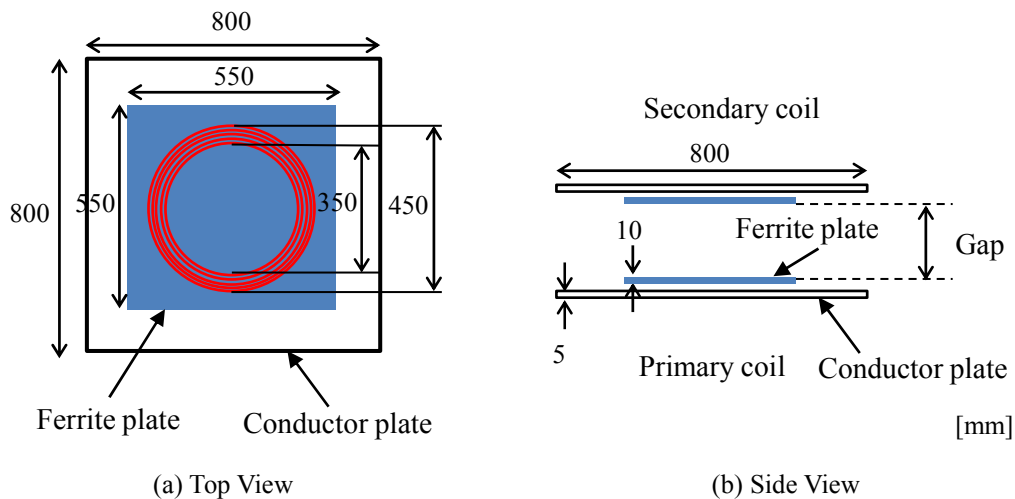


Fig. 4 Configuration of coil (C-Coil).

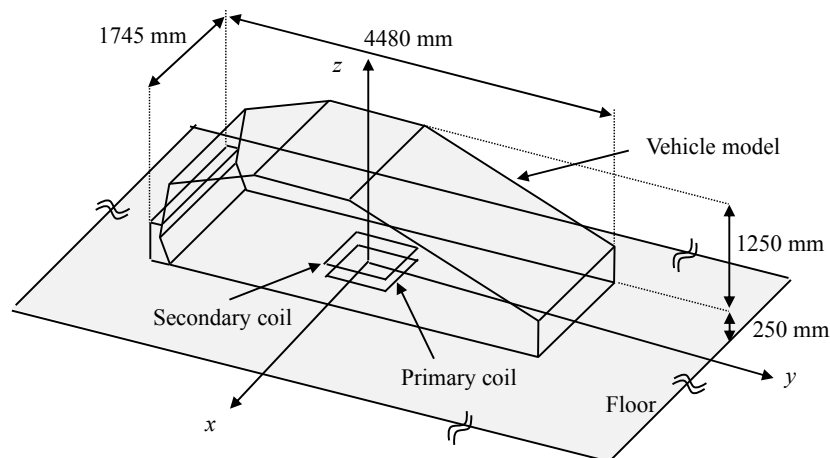


Fig. 5 Analysis model of vehicle.

secondary coil, respectively, Z_1 is the output impedance of the matching circuit in the primary side, Z_2 is the input impedance to the matching circuit in the secondary side, and k is the coupling coefficient between the primary and secondary coils. In this

calculation, the following were taken as unified conditions for comparison: (a) the same frequency, (b) the same transmission power, and (c) the optimum input and output impedance value (the value of the input and output impedance is at maximum efficiency). Under such conditions, coil misalignment changes inductance L_1 , inductance L_2 , and coefficient k . That is, under the condition of the same transmitted power, the current value in the primary/secondary coil changes due to the misalignment. In the HFSS™ program used to calculate the magnetic field intensity distribution, the current value of the coil is set as the excitation source of the magnetic field, so the current value was obtained from the equations described below.

In this circuit, when $L_1 \approx L_2$ and $C_1 \approx C_2$, the resonance frequency is expressed by Eq. (1). The matching condition of impedance at resonance frequency is expressed by Eq. (2).⁽⁴⁾

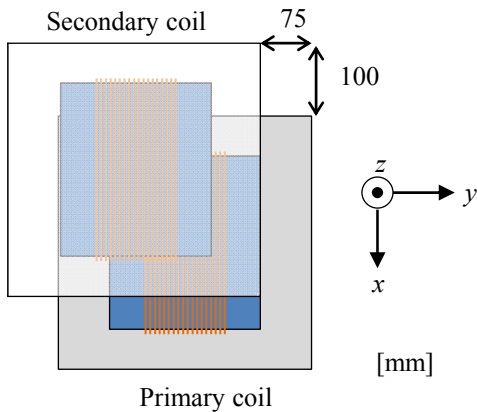


Fig. 6 Maximum permitted horizontal translation of coil position (S-coil).

$$f \approx \frac{1}{2\pi\sqrt{L_1 C_1}} \quad (1)$$

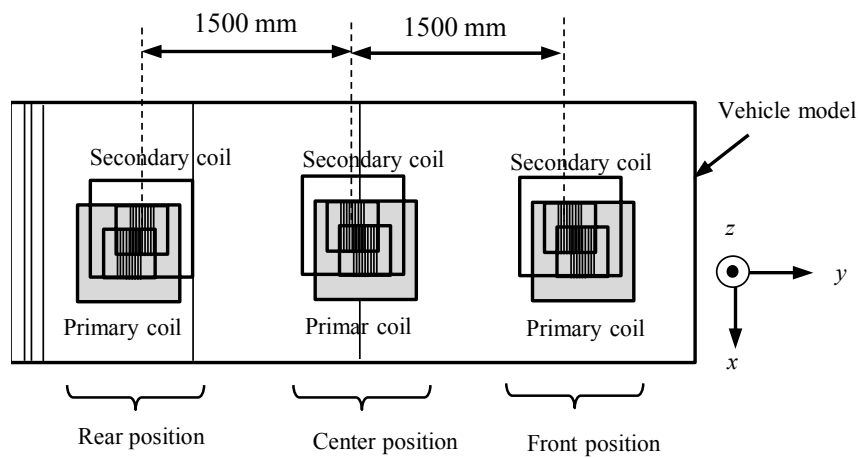


Fig. 7 Coil position on vehicle (S-coil).

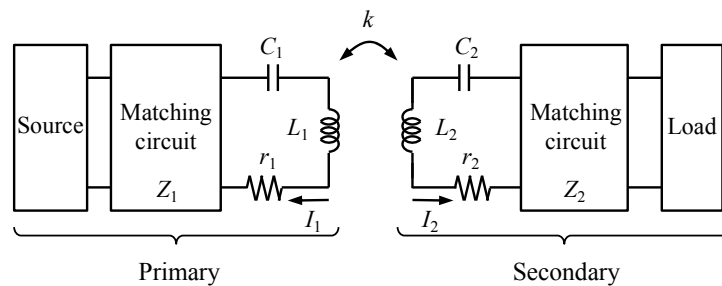


Fig. 8 Circuit topology of WPT system.

$$Z_1 \approx Z_2 \approx k \sqrt{\frac{L_1}{C_1}} \quad (2)$$

Therefore, Z_1 and Z_2 in Eq. (2) are the input and output impedances in condition (c) described above. Next, the current amplitudes of the primary and secondary coils at the transmission power P are given by the following equations derived from Eq. (2):

$$|I_1| \approx |I_2| \approx \sqrt{\frac{P}{Z_1}} \quad (3)$$

$$I_2 \approx -jI_1 \quad (4)$$

Here, Eq. (4) shows the phase relationship between the primary coil and the secondary coil, and the current phase of the secondary coil is delayed by 90° compared to that of the primary coil.

The resonance frequency f_0 at the time of transmission is 85 kHz; the transmission power P is 3 kW; and the current value is calculated from L_1 , L_2 , k , and the above equations. The calculated current values are shown in **Table 1**.

5. Analysis of Magnetic Field Strength

In this section, magnetic field strength was analyzed for evaluation against the reference level.

5.1 Comparison of Magnetic Field Distribution due to Difference in Coil Shape

Figures 9(a) and **(b)** show magnetic field distributions in the xy -plane at $z = 120$ mm of S coil and C coil, as calculated by electromagnetic field simulation for the case where the primary and secondary coils are aligned. Here, the position of $z = 120$ mm is intermediate between the primary coil and the secondary coil. The distribution on line AB, which is a position 20 cm away from the vehicle (the distance of closest approach) is also shown in the

Table 1 Current of coil $|I_1|$ ($= |I_2|$).

Type of coil	Aligned (A)	Misaligned (A)
S-coil	15.5	17.3
C-coil	15.2	20.3

lower part of the figure. The magnetic field strength levels are highest around the coil center for both the S coil and the C coil, and their maximum values are 6.53 A/m and 0.06 A/m, respectively.

Figures 10(a) and **(b)** show the magnetic field distribution in the xy -plane at $z = 120$ mm of the S coil and the C coil, as calculated for the misalignment case. The magnetic field strength levels of both the S coil and the C coil increase with respect to the alignment case, and the maximum values are 8.79 A/m and 4.96 A/m, respectively. These levels are 1.35 and 82.7 times, respectively, higher than the values for the alignment case, with a remarkable degree of increase for the C coil. However, the magnetic field strength level of the C coil is still smaller than that for the S coil, by 0.56 times. The maximum magnetic field strength levels under these conditions are much lower than 21 A/m, which is the “reference level” in ICNIRP 2010.

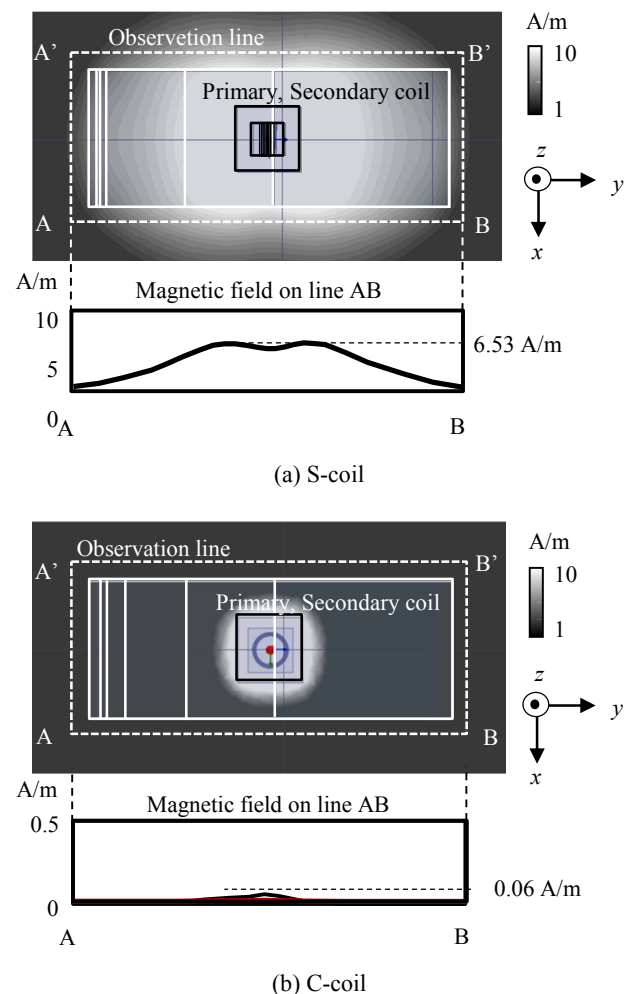


Fig. 9 Magnetic field distribution of aligned case ($z = 120$ mm, xy -plane).

5.2 Comparison of Magnetic Field Distribution Due to Difference in Mounting Position

This section reports results of the magnetic field distribution for the three coil mounting positions described in Sec. 4.2. Magnetic field distributions of the S coil and C coil under each mounting condition obtained by electromagnetic field simulation are shown in **Figs. 11(a) to (c)** and **Figs. 12(a) to (c)**, respectively. From the results of the previous section, since the magnetic field strength is larger in the case of misalignment, only the calculation results in the case of misalignment are shown here. In these figures, the magnetic field distribution on the yz -plane (on the line AB and the line A'B' in Fig. 9) and the zx -plane (on the line AA' and the line BB' in Fig. 10) within the range of $z = 0$ to 500 mm at the position 20 cm away from the vehicle body is shown. The point P indicates the maximum magnetic field strength for each position.

Table 2 shows the values of the magnetic field strength at point P for each coil and position. It was found that the maximum magnetic field strength and its position change depending on the mounting position, and the leakage magnetic field tends to increase in the front or rear position, and this tendency was remarkable in the case of the S coil. Because the magnetic moment vector of the S coil is oriented along the vehicle's front-rear axis, the leakage magnetic field is also stronger along the front-rear axis. Under the conditions of this study, the field strength at point P was in the range of 0.22 to 0.62 times the "reference level" value of 21 A/m, which means that the guideline is met. However, the S coil field might easily exceed the "reference level" when the transmitted power is increased.

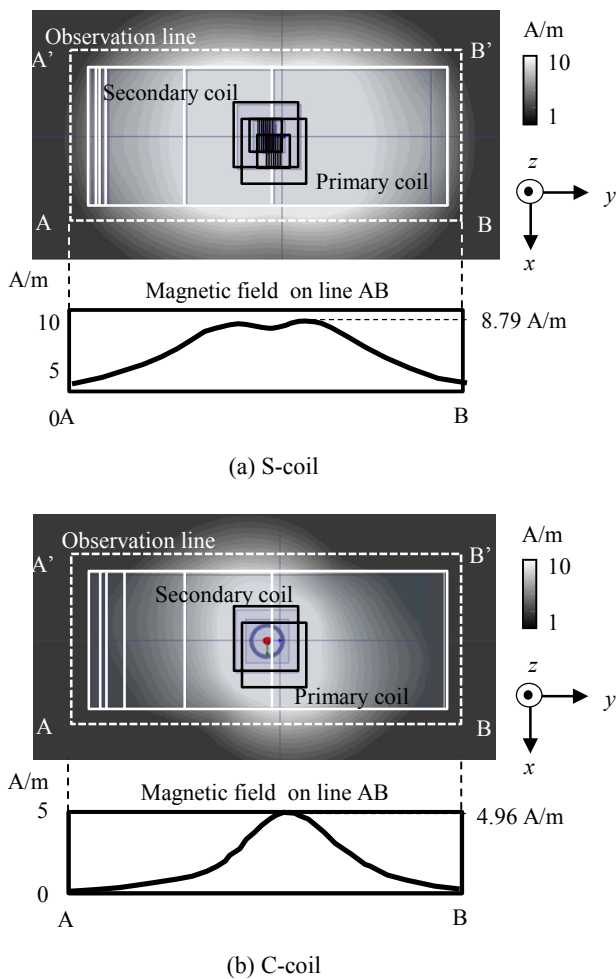


Fig. 10 Magnetic field distribution of misaligned case ($z = 120$ mm, xy -plane).

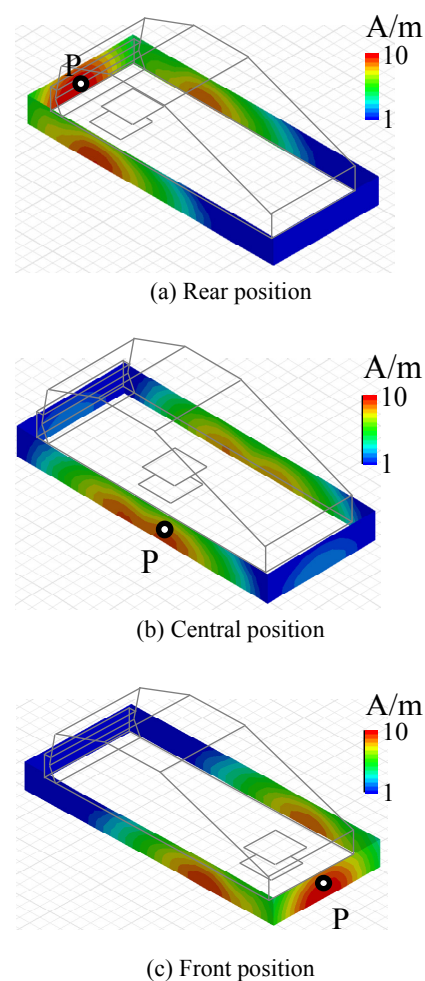


Fig. 11 Magnetic field distribution around the vehicle (S-coil).

6. Analysis of Induced Electric Field

In this section, the electric field induced in the human body is analyzed for evaluation against the “basic restriction”. As described in Sec. 3, the induced electric field is calculated using the result of the magnetic field obtained in the previous section as an input value. As shown in **Fig. 13**, the human body model was placed at point P, where the magnetic field strength is the maximum in each coil arrangement, and the rectangular cuboid magnetic field surrounding the human body was input. **Figures 14** and **Fig. 15** show the induced electric field distributions calculated by the SPFD method under these conditions for the S coil and C coil, respectively. These distributions represent the value of the cross section including the z-axis passing through the center of the ankle. From these results, it was found that the electric field induced in the body was smaller

in the case of the C coil than for the S coil.

ICNIRP 2010 recommends using a percentile value when quantitatively evaluating the induced electric field in the body. This is aimed at eliminating errors included in numerical calculations and is commonly used as a method of influence analysis in the human body. In this evaluation, a 99.9th percentile value is used with reference to the evaluation method of Hirata et al.⁽⁹⁾ **Table 3** shows the calculation results of this percentile for the induced electric field. In the case of the S coil, it was 2 to 3 times higher than for the C coil, and it was higher in the front or rear position than in the center position. The induced electric fields under these conditions are in the range of 0.003 to 0.027 times the basic restriction value of 11.48 V/m in ICNIRP 2010, which is much lower in both cases. In addition, it is clear that the value of “reference level” is quite excessively defined from the comparison result with the “reference level” shown in the previous section.

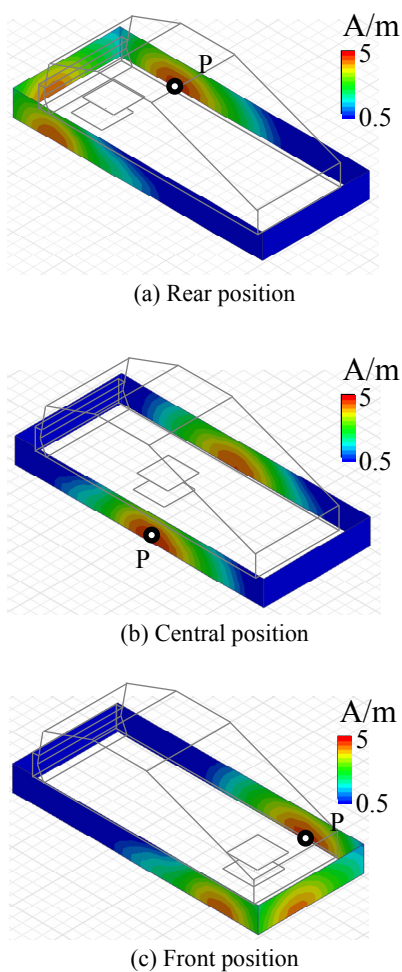


Fig. 12 Magnetic field distribution around the vehicle (C-coil).

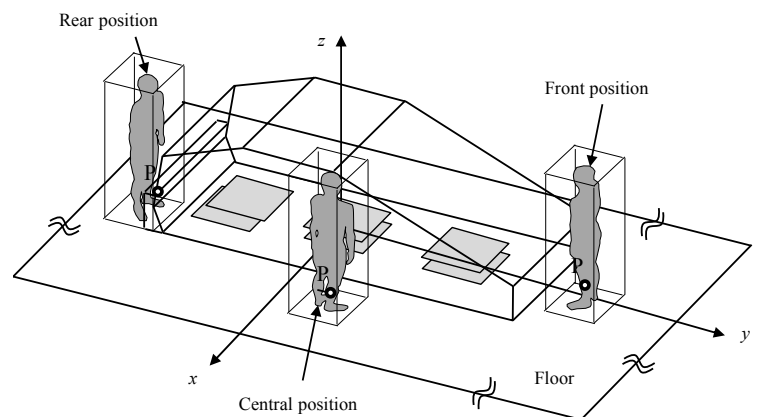


Fig. 13 Position of the human body (S-coil).

Table 2 Magnetic field strength at P.

Type of coil	Rear position (A/m)	Central position (A/m)	Front position (A/m)
S-coil	13.1	8.79	12.4
C-coil	4.96	4.70	4.78

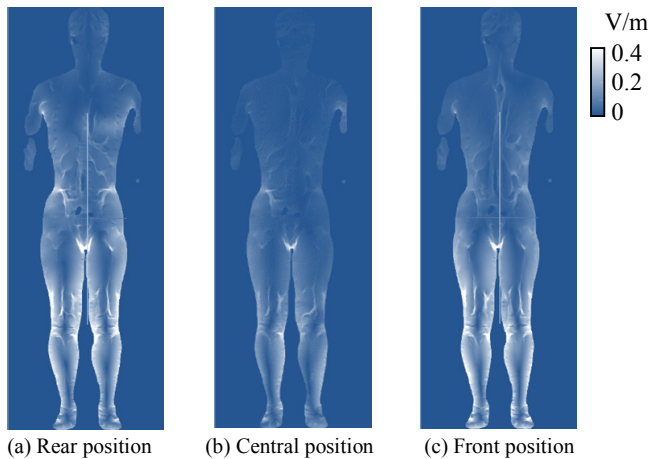


Fig. 14 Induced electric field in human body (S-coil).

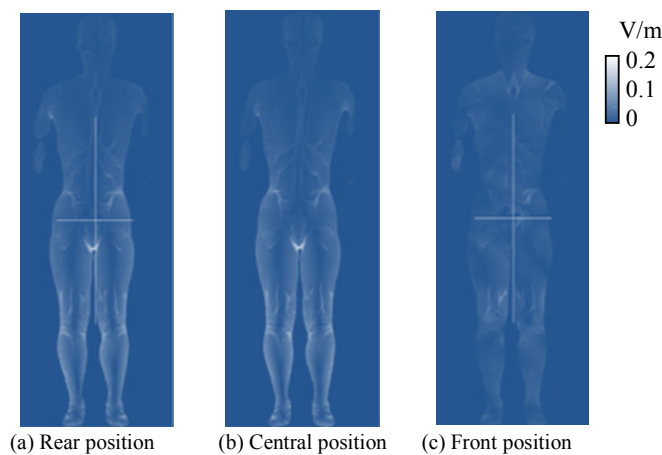


Fig. 15 Induced electric field in human body (C-coil).

Table 3 99.9th percentile of induced electric field in human body.

Type of coil	Rear position (V/m)	Central position (V/m)	Front position (V/m)
S-coil	0.31	0.18	0.28
C-coil	0.07	0.08	0.04

7. Conclusion

We used electromagnetic field simulation to evaluate the exposure to the human body from magnetic field leakage from a WPT system when it is installed in an actual vehicle and a person is standing near the vehicle, which is a reasonable usage scenario. In the comparison between the S coil and C coil, it

was found that the leakage magnetic field from the S coil is larger than that from the C coil. For different mounting positions, the leakage increased when the coil was mounted in the front and rear for both coil types, and this increase was large for the S coil. Under the conditions of this study, it was found that the magnetic field was lower than the ICNIRP “reference level” in all cases.

It was found that the induced electric field strength of the S coil was high, as it was for the leakage magnetic field strength. For the different mounting positions, it was found that the induced electric field became higher for the S coil mounted in the front or rear position. Under the conditions of this study, it was found that the induced electric field was significantly lower than the ICNIRP “basic restriction” in all cases.

References

- (1) Kurs, A., Karalis, A., Moffatt, R., Joannopoulos, J. D., Fisher, P. and Soljačić, M., “Wireless Power Transfer via Strongly Coupled Magnetic resonances”, *Science*, Vol. 317, No. 5834 (2007), pp. 83-86.
- (2) ICNIRP, “Guidelines for Limiting Exposure to Time-varying Electric, Magnetic and Electromagnetic Fields (up to 300 GHz)”, *Health Phys.*, Vol. 74, No. 4 (1998), pp. 492-522.
- (3) ICNIRP, “Guidelines for Limiting Exposure to Time-varying Electric and Magnetic Fields (1 Hz to 100 kHz)”, *Health Phys.*, Vol. 99, No. 6 (2010), pp. 818-836.
- (4) Ishida, M. and Watanabe, T., “Analysis of Effects from Proximate Objects of Inductive Coils for Wireless Power Transfer”, *Proc. EVTeC & APE JAPAN* (2014), No. 20144024.
- (5) Laakso, I., Tsuchida, S., Hirata, A. and Kamimura, Y., “Evaluation of SAR in a Human Body Model Due to Wireless Power Transmission in the 10 MHz band”, *Phys. Med. Biol.*, Vol. 57, No. 15 (2012), pp. 4991-5002.
- (6) Dawson, T. and Stucky, M. A., “High-resolution Organ Dosimetry for Human Exposure to Low-frequency Magnetic Fields”, *IEEE Trans. Magnetics*, Vol. 34, No. 3 (2002), pp. 708-718.
- (7) Nagaoka, T., Watanabe, S., Sakurai, K., Kunieda, E., Watanabe, S., Taki, M. and Yamanaka, Y., “Development of Realistic High-resolution Whole-body Voxel Models of Japanese Adult Males and Females of Average Height and Weight, and Application of Models to Radio-frequency Electromagnetic Field Dosimetry”, *Phys. Med. Biol.*, Vol. 49, No. 1 (2004), pp. 1-15.
- (8) Gabriel, S., Lau, R. W. and Gabriel, C., “The Dielectric Properties of Biological Tissues:

III. Parametric Models for the Dielectric Spectrum of Tissues”, *Phys. Med. Biol.*, Vol. 41, No. 11 (1996), pp. 2271-2293.

- (9) Hirata, A., Ito, F. and Laakso, I., “Confirmation of Quasi-static Approximation in SAR Evaluation for a Wireless Power Transfer System”, *Phys. Med. Biol.*, Vol. 58, No. 17 (2013), pp. N241-249.

Figs. 2-5, 8, 12-13 and 15

Reprinted from SAE Tech. Pap. Ser., No. 2016-01-1158 (2016), Watanabe, T., Ishida, M., Study on the Influence of the Magnetic Field and the Induced Electrical Field in Human Bodies by EV/PHV Wireless Charging Systems, © 2016 SAE International, with permission from SAE International.

Figs. 3, 6-7, 9-11 and 14

Reprinted from Proc. EVTeC and APE Japan (2016), No. 20169021, Watanabe, T., Ishida, M., Study on the Influence of the Magnetic Field and the Induced Electrical Field in Human Bodies by Wireless Charging Systems, © 2016 JSAE, with permission from Society of Automotive Engineers of Japan.

Toshiaki Watanabe

Research Fields:

- Electromagnetic Analysis
- Mobile Antenna
- Wireless Power Transfer
- Mm-wave Radar System



Academic Societies:

- The Institute of Electronics, Information and Communication Engineers
- The Institute of Electrical Engineers of Japan
- Society of Automotive Engineers of Japan

Masaya Ishida

Research Fields:

- Electromagnetic Analysis
- Wireless Power Transfer
- Microwave Circuit



Academic Societies:

- IEEE
- The Institute of Electronics, Information and Communication Engineers
- The Institute of Electrical Engineers of Japan
- Society of Automotive Engineers of Japan